IMAGING AND MOTION PREDICTION FOR
AN AUTOMATED LIVE-BIRD TRANSFER PROCESS

Kok-Meng Lee, Jeffry Joni and **Xuecheng Yin**
The George W. Woodruff School of Mechanical Engineering,
Georgia Institute of Technology
Atlanta, GA 30332-0405
Tel: (404)894-7402; Fax: (404)894-9342; email: kokmeng.lee@me.gatech.edu

ABSTRACT

This paper presents the illumination design of a real-time live-bird imaging system for determining the size and initial presentation of a bird on a moving conveyor. A real-time live-bird imaging system presents a challenging design problem, for it must minimize the variability of the birds' visual reflexes to mechanical processes, it must account for variations in bird size/shape/color, it must meet the cycle-time requirement, and yet provide an adequately illuminated environment to ease human supervision. In this paper, we first identify the variables needed for motion prediction. Second, by analyzing the bird visual perception we have developed a two-stage structured illumination that has the potential to minimize the demand on the control efforts of the transfer system, and to improve birds' welfare and the ultimate product quality. Finally, we present the image algorithms and experimental results of the design evaluation using live birds. It is expected that the design principles presented in this paper provide essential bases for motion analysis, prediction, and control of an automated live-bird transfer process.

1. INTRODUCTION

Manual handling of live birds is a hazardous and unpleasantness task. There are potentials for a variety of injuries to human handlers since the birds tend to flail about when they are caught. Potential injuries include cuts/scratches which can easily become infected in that environment, a variety of respiratory and visual ailments resulting from the high level of dust and feathers that come off the birds, hand or finger caught in the moving shackle line at the processing plant, and cumulative trauma disorders due to repetitive motion. The unpleasantness of this task sometimes results in high employee turnover rates at some plants, which requires constant retraining of new employees. In addition, it is also extremely difficult to attract new workers to the job. This makes handling live-birds an ideal candidate for automation since the potential benefits and payback for such systems derive from a reduction in labor costs and a potential reduction of bruising and downgrading of birds.

Despite the need for automation, live birds have always been handled manually (from hatching through processing). The reason for this is that the handling of live birds presents unique challenges, such as the following: (1) Unlike handling of non-reactive objects, both the mechanical forces and the bird's natural reflexes contribute to the overall dynamics. (2) Live birds vary in size and shape, making handling automation difficult. (3) Since both the birds and the grasping fingers are compliant, contact forces depend on the surface geometries and are position/orientation dependent. (4) In order to justify the need for automation from a cost-saving viewpoint, the mechanical devices must perform the repetitive task in a shorter amount of time, and with more accuracy than a human.

To address the challenges of handling live-birds for processing, Georgia Tech and the University of Georgia have jointly conducted a research project to develop methods of transferring live birds from a conveyor to a moving shackle line. Their efforts have led to the development of a compliant moving grasper (Lee, 1999; Lee *et. al*, 1999), and an automated leg locating and transferring system (Lee, 2000) that uses the velocity difference between the bird's body and its feet to manipulate the leg kinematics of the birds. Prior studies suggest that in order to increase the success rate of inserting both legs of the bird into the shackle at high speed, a means to predict the time trajectory of the leg motion is essential. In addition, it is desired to keep the variability of the birds' initial postures and natural reflexes to mechanical processes as uniform as possible in order to minimize demands on the control efforts of the transfer system, and to improve birds' welfare and the ultimate product quality. To achieve these objectives, non-evasive techniques must be developed based on the study of stimulus environments to promote behavior compliance, on the study of the role of visual responsiveness, and on the evaluation of vision acuity in different spectral environments. Such real-time control application requires a stringent combination of structured illumination, reflectance, imaging sensor and computation. For these reasons, we explore methods of designing an imaging system using structured illumination that is insensitive to the birds' visual response and yet, that provides sufficient information to predict the bird's motion as the bird is moving through the grasping mechanism.

The remainder of the paper is organized as follows: We begin with a brief overview of the high-speed live-bird transfer mechanism. Along with the governing equations that illustrate the operating principles, we highlight the essential variables needed for to control the bird's leg kinematics for insertion. We discuss the imaging system design in Section 3. On the basis of the bird's visual perception, a two-stage structured illumination system design and the image-processing algorithms for inferring the bird's direction and initial presentation are presented. The design has been evaluated experimentally with live birds, and

the results are summarized and discussed in Section 4, followed by the conclusions given in Section 5.

2. THE TRANSFER MECHANISM

Figure 1 shows the prototype live-bird transfer system developed at Georgia Tech, which consists of a body grasper, an inclined conveyor, and a shackle-inverter mechanism. In operation, the birds are fed in a single file on the down-inclined conveyor toward the body grasper, which is essentially a pair of drums filled with flexible fingers. The two drums, rotated at the same speed but in the opposite direction, move the bird toward the shackle inverter as shown in Figure 1(c) while the fingers continuously constrain the bird by its body. Once the legs are inserted in the grippers, both the bird and the shackle are free to travel together until they reach the end of the conveyor, at which the momentum along with the gravity causes the bird to rotate with the shackle.

(a) side view (b) front view (c) shackle inverter
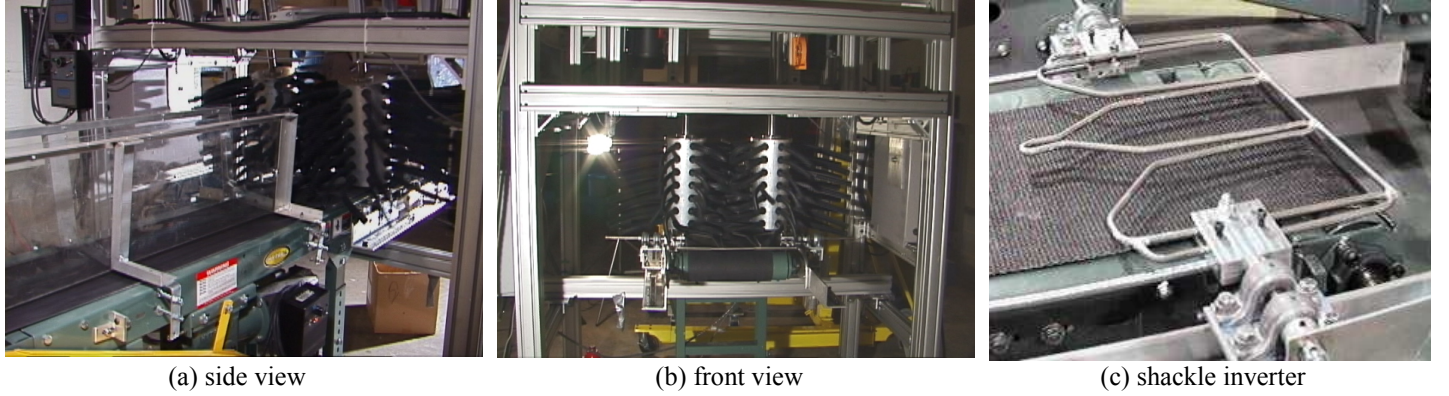
Figure 1 Automated transfer mechanism

The reference coordinate frame XYZ is assigned at the intersection between the rotating axis of the drum and the conveyor surface as shown in Figure 2, where the X- and Y-axes are directed along and perpendicular to the conveyor surface respectively.
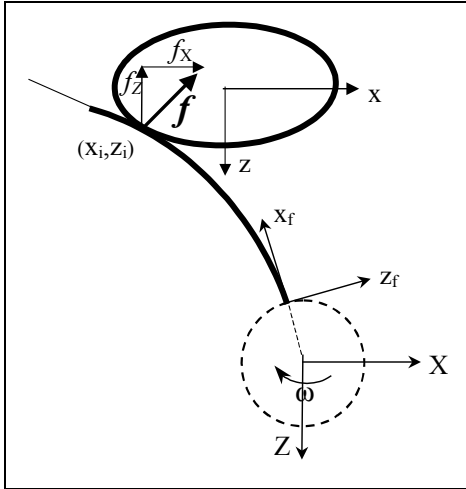
Figure 2 Kinematic model of the finger/bird interaction

When the drum rotates, the finger exerts a force f at the contact point $(x_i,\ z_i)$ on the bird, which is modeled as an ellipsoid:

$$\frac{x^2}{\eta^2}+\frac{y^2}{\lambda^2}+\frac{z^2}{\gamma^2}=1 \qquad (1)$$

where η, λ, and γ are characteristic radii of the ellipsoid. As shown in Figure 2, the cross-section intercepted by the rotating finger at $y=y_i$ ($|y_i|<\lambda$) is essentially an ellipse:

$$\frac{x^2}{a_s^2}+\frac{z^2}{b_s^2}=1 \qquad (2)$$

where $a_s^2=\eta^2[1-\frac{y_i^2}{\lambda^2}]$ and $b_s^2=\gamma^2[1-\frac{y_i^2}{\lambda^2}]$.

With a pair of drums, the Z-component of the contact force, f_Z, provides the compliant force to grasp the bird while the X-component, f_X, pushes the bird toward the awaiting shackle.

Figure 3 illustrates the leg kinematics of a bird on a moving conveyor, where ℓ_1 and ℓ_2 are the lengths of the lower and upper limbs respectively; φ_1 and φ_2 are the joint angles of ℓ_1 and ℓ_2 respectively; and J_1, J_2 and J_3 are the ankle, hock, and knee joints respectively. The joint angles can be determined from Equations (3) and (4) using the law of cosines:

$$\varphi_2=\cos^{-1}\frac{\ell_1^2+\ell_2^2-(X_{31}^2+Y_{31}^2)}{2\ell_1\ell_2} \qquad (3)$$

$$\varphi_1=\tan^{-1}\frac{Y_{31}}{X_{31}}-\tan^{-1}\frac{\ell_2\sin\varphi_2}{\ell_1-\ell_2\cos\varphi_2} \qquad (4)$$
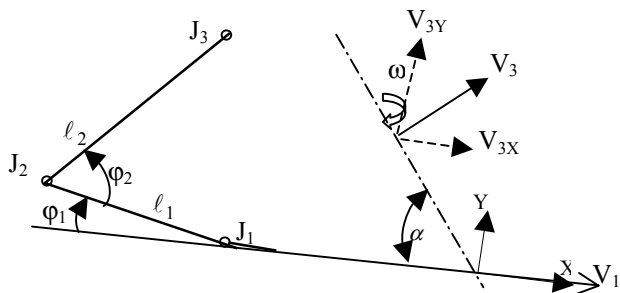
Figure 3 Leg kinematics on moving conveyor

We note that as birds tend to keep their feet in contact with the conveyor, joint 1 travels with the conveyor at a velocity V_1. The bird body, grasped between the fingers-filled drums and hence at the hip joint, is translated at a velocity V_3 that has a direction perpendicular to the rotating axis. Thus, the legs can be manipulated by appropriately controlling the drum velocity with respect to that of the conveyor. Unlike the traditional articulated robotic arm where the actuation is applied directly through the joint angles, the live object can only be manipulated indirectly. The velocity difference between joint 1 and joint 3 causes a change in leg kinematics:

$$\begin{bmatrix} \ell_1 \sin\varphi_1 + \ell_2 \sin\varphi_{21} & -\ell_2 \sin\varphi_{21} \\ \ell_1 \cos\varphi_1 - \ell_2 \cos\varphi_{21} & \ell_2 \cos\varphi_{21} \end{bmatrix} \begin{bmatrix} \dot{\varphi}_1 \\ \dot{\varphi}_2 \end{bmatrix} = \begin{bmatrix} V_{3X} - V_1 \\ V_{3Y} \end{bmatrix} \quad (5)$$

where V_{3X} and V_{3Y} are the X and Y velocity components of V_3 respectively; and $\varphi_{21} = \varphi_2 - \varphi_1 = -\varphi_{12}$. Equation (5) provides a means to determine the kinematical relationship for presenting the legs of the bird to the shackle inverter. Equation (5), a non-linear differential equation, can be numerically solved for the leg's motion, $\varphi_1(t)$ and $\varphi_2(t)$, for a given conveyor inclination with respect to the drum axis.

The presentation of the legs at the exit of the grasper depends on the bird's initial posture $\varphi_1(t=t_i)$ and $\varphi_2(t=t_i)$ as well as the bird's size and the drum speed. In order to lift the hocks of the bird and insert its legs into the grippers, it is necessary to determine the size and initial posture of the bird in real-time so that the drum speed can be appropriately controlled.

3. IMAGING SYSTEM DESIGN

It is desired to minimize the variability of the birds' initial postures and natural reflexes to mechanical processes in order to minimize the demands on the control efforts of the transfer system. Prior experimental studies using live birds have suggested that a uniform "sitting" posture can be obtained when the birds are placed on a moderately inclined conveyor in total darkness. To ease human supervision of the automated live-bird transfer operation, it is desired to design the vision system with a structural illumination in the visible range of human eyes but with a light spectrum to which birds are not sensitive.

3.1 Review of Bird Visual Perception

Behavioral experiments for color vision in birds began with the work of Hess (1912). He sprinkled grain on a floor and illuminated it with the six colors projected in a spectrum. He reported that the chickens ate the grain illuminated by red, yellow, and green light not the grain illuminated by the blue and violet light. Watson (1915) and Lashley (1916) have shown that the chick's spectral limits are from 700-715nm at one end of the spectrum and 395-405nm at the other. The maximum sensitivity of the chick eye is at 560nm and that of the adult fowl at 580μm. Later, Honigmann (1921) and others, working with both stained and illuminated rice grains, observed that chickens did eat the blue and violet grains, albeit less avidly than they did the others. Using pigeons, Armington and Thiede (1956) demonstrated that birds have a Purkinje shift (a change in peak spectral sensitivity from scotopic to photopic vision) similar to that of humans. The eye of the pigeon subjected to darkness for at least 45 minutes, becomes dark-adapted and responds maximally to light at 534nm and up to 664nm. The spectral range for the light-adapted eye is 424-704nm with the maximum response to 565nm.

Until the 1950's, most avian vision was studied using psychophysical and anatomical experimental approaches. Modern visual science provides abundant empirical evidence that the retina (the innermost tissue layers of the eye) sends a complex neural signal to the brain. The photoreceptors fall into two categories: *rods* provide nighttime vision and *cones* provide daylight vision. Both rods and cones contain photosensitive pigments. These photo-pigments absorb light quanta and convert this light energy into electrical activities, which is the first step in a sequence of events that ultimately leads to vision. The use of this neuro-physiological approach has led to a better understanding of the *scotopic* and *photopic* vision. Scotopic vision is defined as vision that occurs under dim or nighttime conditions, under which the rods dominate the retina. On the other hand, the cones dominate the retina under *photopic* lighting conditions, which is defined as vision under bright (daylight) lighting conditions. Rods contain the photo-pigment *rhodopsin* (also known as visual purple). To determine scotopic spectral sensitivity, the subject is dark adapted for 45 minutes; the threshold (the minimum amount of energy required) for the subject to detect stimuli of various wavelengths is determined; and the sensitivity curve is simply the reciprocal of the threshold function. This scotopic spectral sensitivity curve has essentially the same form as the rhodopsin absorption spectrum (Wald, 1945). This similarity in form suggests that the scotopic spectral sensitivity function is determined by the rhodopsin absorption characteristics.

Birdspectral sensitivity

Using published results; Kare and Rogers (1976) compared the chicken rhodopsin and iodopsin adsorption spectral of visual pigments in the chicken with the retinal spectral sensitivity of light-adapted and dark-light pigeons. The iodopsin is a violet, light-sensitive pigment found in the retinal cones of the eye. The results, as shown in Figure 4, were obtained micro-spectrophotometrically by inserting microelectrodes into the retina after removal of lens and cornea. The scotopic data are from Donner (1953), the photopic data from the same source (barred circles) and from Granit (1959) (open circles).

As shown in Figure 4, the scotopic sensitivity agrees well with the absorption spectrum of rhodopsin. The photopic sensitivity is displaced about 20μm toward the red from the absorption spectrum of iodopsin. The cones of most avian retinas contain brightly colored oil droplets in their inner segments, immediately adjacent to the outer segments. Therefore most light reaching the outer segments has probably passed through a corresponding oil drop. This anatomical arrangement has led to the suggestion that the droplets (orange, yellow, or red) act as intraocular light filters, intensifying similar colors but reducing the discrimination of others such as violets and blue (Portmann, 1950). Figure 4 suggests that the peak scotopic vision of chicken is similar to that of the human at about 507nm. Although both chicken and human photopic vision have maximal quanta absorption at 565nm, the human photopic spectral sensitivity curve has a broad peak from 400nm to 700nm (Wald, 1945).
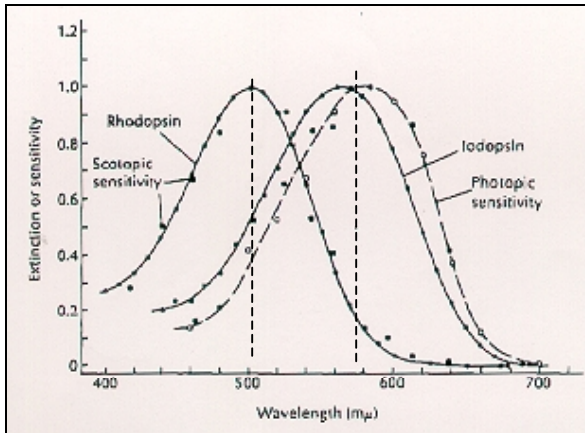
Figure 4 Absorption spectra of chicken rhodopsin and iodopsin, compared with the retina spectral sensitivity of dark- and light-adapted pigeons (Kare and Rogers, 1976).

Dark-adaptation characteristics

After exposure to an adapting light, rods and cones recover sensitivity at different rates. The cone pigments recover from bleaching at a faster rate than do the rods. It takes approximately 1.5 minutes for 50 percent of a cone photo-pigment to recover following bleaching (Rushton, 1963b). The gradual improvement in vision is referred to as dark adaptation. A typical human dark adaptation curve is shown in Figure 5 (adapted from Hecht *et al*, 1942). The curve was generated by exposing the person to a bright-adapting light to bleach most of his/her photo-pigment and determining the detection threshold as a function of time for stimuli flashed against a totally dark background.
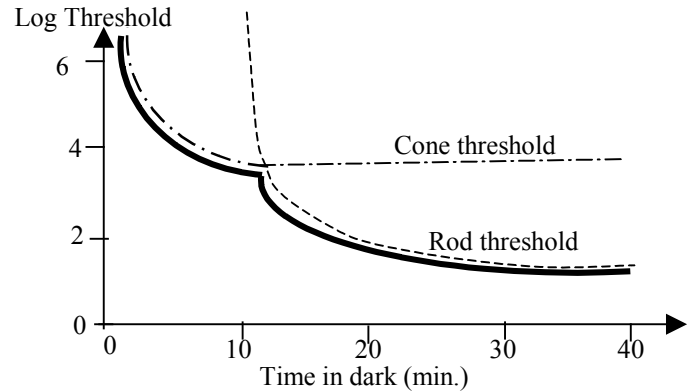
Figure 5 Typical dark adaptation curve (with a 420nm stimulus)

As shown in Figure 5, over a period of about 35 minutes, threshold improves by about 5 log units (or 100,000 times more light sensitive). The curve has two distinct sections: The first section shows a rapid reduction in threshold up to about 5 minutes, where the curve plateaus. This portion of the dark adaptation curve represents cone thresholds (dash-dot line). At about 10 minutes, there is an abrupt change in the slope of the curve (Hecht *et al*, 1937) followed by a slow reduction in threshold up to about 35 minutes due to the detection by the rods (dash line). When the dark adaptation curve was obtained with a stimulus of 650nm, the rod aspect is missing and the result is consistent with the scotopic vision in Figure 4, which shows that the photo-chromatic interval for 650nm is nearly zero.

A two-stage structured illumination is considered here to meet the stringent requirements of bird vision. The first stage is to cause the bird to be light adapted, and during this period, the bird direction (facing forward or backward) can be determined along with its body width using color vision. In order to keep the bird from flailing and to minimize variation in its presentation as it enters the grasper, we employ the retro-reflective sensing technique with a low-400nm illumination in the second stage to image the posture of the bird on the moving conveyor before it enters the grasping mechanism.

3.2 Bird Direction Detection –light adaptation stage

The direction of the bird, facing forward or backward, is determined from the relative position of the comb with respect to its body. The comb (red) can be distinctively segmented in the RGB color space. However, to reliably detect a variability of combs under practical illumination, we use a three-layer RCE neural classifier model (Reilly, Cooper and Elbaum, 1982) to provide supervised learning of color pattern categories separated by nonlinear, essentially arbitrary boundaries. The concept of a pattern class develops from storing in memory a limited number of class elements (prototypes). Associated with each prototype is a modifiable scalar weighting factor (λ) that effectively defines the threshold for categorization of an input with the class of the given prototype. Learning involves (1) commitment of the prototypes to memory and (2) adjustment of the various λ factors to eliminate classification errors.

As shown in Figure 6, the neural network consists of N inputs, M nodes (storing cells) in the hidden layer, and C output. The hidden layer is initially empty, and the number of cells M increases with training. If the new training pattern does not belong to an existing class (or in other words, not within the sphere defined by λ_k), a new node is created in the hidden layer. The neural network is illustrated by the pseudo-code given in Figure 7.
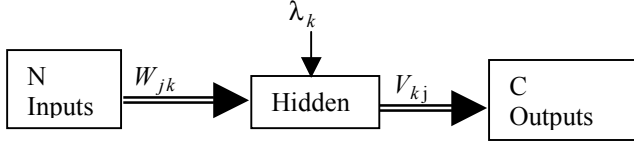
Figure 6 Structure of the trained network

3.3 Initial Posture Determination – dim blue illumination

The structured retro-reflective imaging system consists of a low-intensity spectrally filtered illumination source and a vision system that images the bird against a retro-reflective background. Since the transfer time in the dark adapted environment before entering the grasping mechanism is on the order of 5 seconds, during which the bird's retina is dominated by the cones, we choose the illumination around 420nm. Figure 8 shows the spectral characteristic of the illumination source consisting of four warm-white fluorescent lamps and its corresponding luminance when the lamps are filtered through 1, 2, 3 and 4 layers of Roscolux full-blue filters. Typical coefficient of retro-reflection (candelas/Lux/m^2) is shown in Figure 9, where the observation angle α is between the illumination and observation axes; and the entrance angle β is the angle from the illumination axis to the retro-reflector axis (or the axis perpendicular to the retro-reflective surface).

To determine the initial leg posture from Figure 5, the following assumptions are made:
1. We model the body of the broiler as an ellipsoid as characterized by Equation (1).
2. Based on observation of birds' postures in equilibrium, we approximate the bird's CG at the mid-point between its hip joints.
3. The broilers for a given batch are similar. In other words, the following ratios could be obtained statistically:

$L_1 = \dfrac{\ell_1}{\ell_2}$ and $L_2 = \dfrac{\ell_2}{2\lambda}$ where 2λ is the bird body-height.

4. The bird's orientation (facing forward or backward) is known.

The vision algorithm consists of the following steps:
Step 1: The image is subtracted from the background so that the background is eliminated.
Step 2: The resulting image is histogram equalized in order to stretch contrast for gray levels near histogram maxima and compress those with gray levels near histogram minima. By expanding the contrast for most of the pixels, the transformation significantly improves the detectability of the image features.
Step 3: The blob characterizing the bird is segmented by size, and the outline of the blob is then determined using an edge finding routine.
Step 4: Using the Hough transformation technique, the center, orientation, and major and minor radii of the ellipse characterizing the bird are obtained.
Step 5: Note that the CG must pass through joint 1 on which the bird's body is supported. The position of joint 1, which is the intersection between the line of gravity and link 1, is determined.
Step 6: From $\ell_2 = 2\lambda L_1$ and $\ell_1 = L_1\ell_2$, the joint angles can be deduced from Equations (6) and (7).

Initialization
Number of nodes on the input layer = N,
Number of nodes on the hidden layer = M = 0,
Number of nodes on the output layer = C.

Training begins
Let the first training pattern be
$$\Gamma_{p1} = \begin{bmatrix} t_{p1}(1) & \cdots t_{p1}(i) \cdots & t_{p1}(N) \end{bmatrix}^T$$
that belongs the jth Class.
Then, the first node in the hidden layer is constructed as follows:
$$W_{j1}(i) = t_{p1}(i) \qquad \text{where } i = 1, \ldots, N,$$
$$V_{1j} = 1, \text{ and}$$
$$\lambda_1 = default\ threshold.$$
The process repeats and new hidden cells are created.

Classification
There will be M cells available when the nth training pattern that belongs to the jth Class arrives.

For $k = 1:M$,
$$g_k = N_{\lambda k}\left(D(W_k, \Gamma_{pn})\right)$$
where $D(W_k, \Gamma_{pn}) = \left\| W_k - \Gamma_{pn} \right\|^3$, and
$$N_{\lambda k}(x) = \begin{cases} 1, & x < \lambda_k \\ 0, & x \geq \lambda_k \end{cases}$$
If $g_k = 1$ and $V_{kj} = 1$.
The training pattern is correctly contained within one of the cells, go to the next sample.
End

If $g_k = 1$ and $V_{kj} = 0$.
The classification is incorrect. Decrease λ_k until $g_k = 0$.
End

If $\forall k$, $g_k = 0$, add new cell in the hidden layer.
$$W_{M+1}(i) = t_{pn}(i),$$
$$V_{(M+1)j} = 1, \text{ and}$$
$$M = M + 1$$
End
End

Figure 7 Pseudo-code of the network training
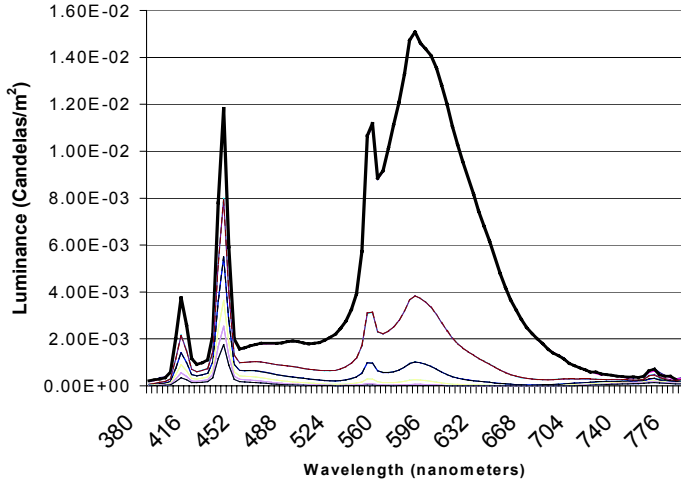
Figure 8 Spectrally filtered blue illumination
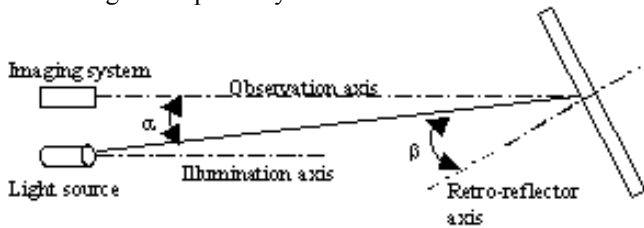
(a)Retro-reflection
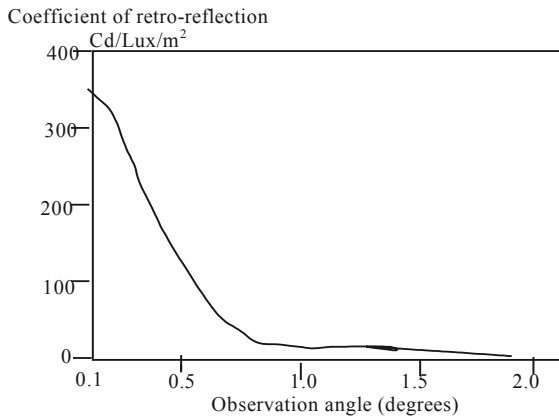
(b) Effect of observation angle
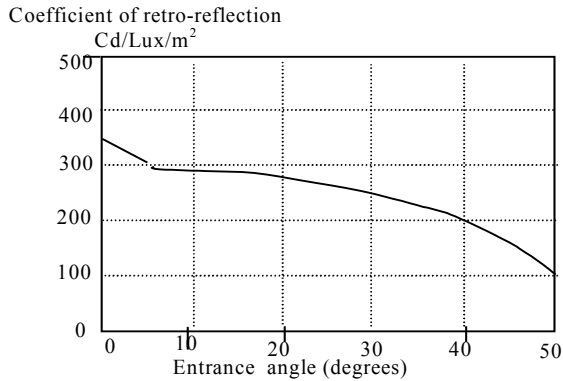
(c) Effect of entrance angle

Figure 9 Schematics illustrating retro-reflective vision sensing

4. EXPERIMENTAL RESULTS

The design has been experimentally tested with live birds using the prototype setup shown in Figure 1. Each of the birds was placed on a six-foot conveyor between two narrowly guided transparent panels. The vision system was triggered by a beam-switch and imaged the bird just before it entered the grasper.

Direction detection

Figure 10 shows the structure of the trained RCE neural network classifier, where the inputs are the RGB components of the sample pixels, and the outputs are the two classes (the comb C and the non-comb NC). The training samples and trained nodes are summarized in Table 1. The original and the computed result using the classifier are compared in Figure 11.
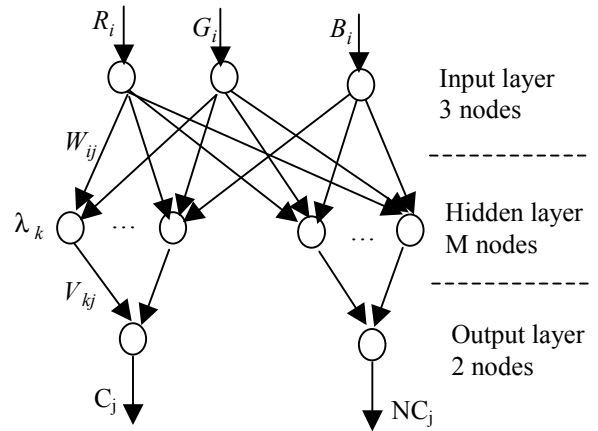
Figure 10 Structure of the trained network

Initial posture determination

Figure 12 shows typical bird postures on a conveyor moving at 0.5m/s toward the grasper. Figure 12(a) shows a typical image of the bird (white feathers) against a retro-reflective background (580-85 Black Scotchlite) with a dim illumination filtered with three layers of Roscolux full-blue filters. Figures 12(b)-(d) illustrate the image processing of the same bird. Typical postures are given in Figures 12(d)-(f) and the computed results are summarized in Table 2, where the orientation of the bird is measured with respect to the conveyor surface.
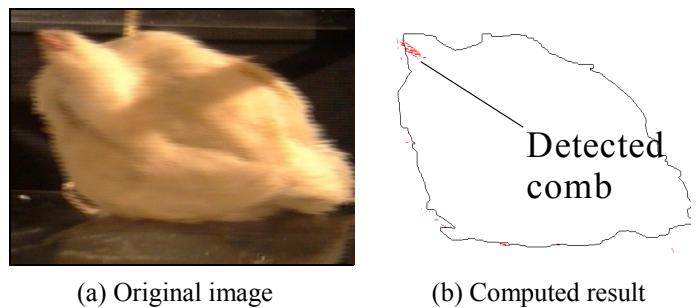
(a) Original image   (b) Computed result

Figure 11 Typical computed result of color classifier

Table 1 RCE Training Samples and Results

Training pairs (R, G, B; Comb)	Training results
93, 33, 18; 1	Number of hidden nodes, M=4
95, 34, 17; 1	
162, 78, 51; 1	Hidden nodes stored:
147, 70, 37; 1	93, 33, 18
154, 85, 52; 1	162, 78, 51
152, 62, 47; 1	147, 70, 37
154, 73, 44; 1	211, 112, 73
164, 75, 42; 1	
102, 42, 19; 1	Maximum prototype (class) threshold:
211, 112, 73; 1	λ_{max}=15

(a) Image of sit posture   (b) Subtract from background

(c) Histogram equalized   (d) Edge-detected sit posture

(e) Typical sit-up posture   (f) Typical stand posture
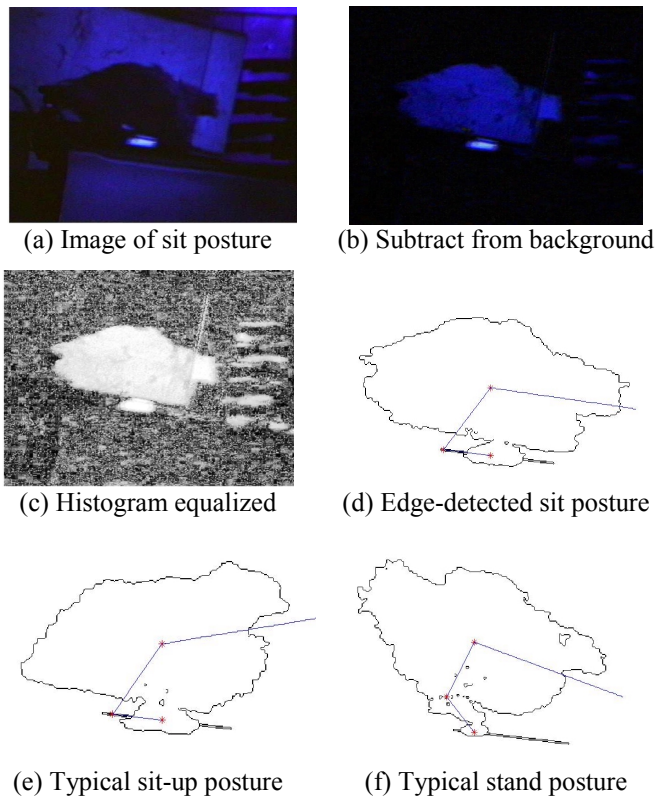
Figure 12 Typical Initial Postures

Table 2 Initial Posture Determination

Initial Posture	ℓ_1 mm (in.)	ℓ_2 mm (in.)	φ_1	φ_2	Body Orientation
Sit	75 (3)	100 (4)	0°	69°	-0.36°
Sit-up	69 (2.75)	94 (3.75)	0°	76.6°	17.25°
Stand	69 (2.75)	94 (3.75)	30°	114°	-12.5°

Effect of illumination on posture variability

Table 3 compares the design against two standard conditions; daylight and in total darkness (Lee, 2000). In each of the treatments, 20 birds were used. Table 3 suggests that the structured illumination can significantly minimize the variability of the initial postures.

Table 3 Entry Postures (conveyor inclination θ=7.5°)

Conveyor speed	V_1=0.375 m/s (15 in./s)		V_1=0.5 m/s (20 in./s)	
Lighting	Day light	In darkness	Blue illumination	
			Male bird	Female bird
sit down	25%	100%	80%	75%
sit up	50%	0%	5%	5%
stand	25%	0%	15%	20%

5. CONCLUSIONS

A practical imaging system design essential for live-bird motion prediction and analysis of an automated live-bird transfer process has been presented. The two-stage structured illumination system decouples the direction detection from the initial posture determination. The first stage, during which the bird adapts to daylight, uses a neural network color classifier to detect the direction of the bird. The initial posture of the light-adapted bird is then determined using a retro-reflective imaging technique. The concept feasibility of the imaging method has been experimentally demonstrated with live birds. Work has been directed toward evaluation of this imaging system in real-time control of the transfer system.

REFERENCES

Armington, I. C. and F. C. Thiede (1956) "Electroretinal Demonstration of a Purkinje Shift in the Chicken Eye." *Am. I. Physiol.* 186, 258.

Dooner, K. O. (1953), "The Spectral Sensitivity of the Pigeon's Retinal Elements." *J. Physiol.*, 122, 524.

Granit, R. (1959) "Neural Activity in the Retina." *in Hb. Of Physiology*, Sect. 1, (H.W. Magoun Ed.) Baltimore: Williams and Wilkins, p. 693.

Heemskerk, W. J. C., (1992) "Method for Causing Sitting Poultry to Stand Up and Apparatus for Carrying Out this Method," *Patent* 5,088,959.

Hess, V. C. (1912) "Gesichtssinn," *Hb. Vergl. Physiol.* 4, 555.

Honigmann, H. (1921), "Untersuchungen über Lichtempfindlichkeiten und Aclaptierung des Vogelauges." *Arch Ges. Physiol.* 189.1.

Keiter, M. E., (1992) "Method and Apparatus for Orienting Live Poultry," Patent 5,129,857.

Kettlewell, P. J. and M. J. Turner, (1985) "A Review of Broiler Chicken Catching and Transport Systems," *J. of* Agricultural Engineering Research, Vol. 31, pp. 93-114.

Lashley, K. S. (1916) *The Colour Vision of Bird: the Spectrum of the Domestic Fowl.*

Lee, K.-M., (1994) "Design Concept of an Integrated Vision System for Cost-Effective Flexible Part-Feeding Applications," *ASME Journal of Engineering For Industry*, Vol. 116, pp. 421-428, November.

Lee, K.-M., (1999), "On the Development of a Compliant Grasping Mechanism for On-line Handling of Live Objects, Part I: Analytical Model," IEEE/ASME Int. Conf. on Advanced Intelligent Mechatronics (AIM'99), Atlanta, GA, Sept. 19-23.

Lee, K.-M. B. Webster, J. Joni, X. Yin, R. Carey, M. Lacy, R. Gogate, (1999) "On the Development of a Compliant Grasping Mechanism for On-line Handling of Live Objects, Part II: Design and Experimental Investigation," AIM'99, Atlanta, GA, September 19-23.

Lee, K.-M. (2000), "Design Criteria for Developing an Automated Live-bird Transfer System," IEEE Int. Conf. on Robotics and Automation, San Francisco, 22-28 April.

Parker, A. E. Jr., (1974) "Method and *Apparatus* for Handling Live Poultry," US Patent # 3,796,192.

Portmann, A. (1950), Traite de Zoologie," Tome XV. *Les Organes des Sens* (P. P. Graise Ed.) Paris : Masson & Cle., p.273.

Reilly, D. K., L. N. Cooper, and C. Elbaum, (1982) "A Neural Model for Category Learning." *Biological Cybernetics*, Vol. 45, 1982, pp35-41.

Scott, G. B., (1993) "Poultry Handling: A Review of Mechanical Devices and Their Effect on Broiler Welfare," *World's Poultry Sc. J.*, Vol. 49, pp. 44-57.